Chromia–Pillared α–Zirconium Phosphate Materials as Catalysts for Thiophene Hydrodesulfurization

ARTICLE *in* LANGMUIR · FEBRUARY 1999

Impact Factor: 4.46 · DOI: 10.1021/la981446k

3 AUTHORS, INCLUDING:

Enrique Rodriguez-Castellon
University of Malaga

394 PUBLICATIONS **5,210** CITATIONS

SEE PROFILE

Chromia-Pillared α-Zirconium Phosphate Materials as Catalysts for Thiophene Hydrodesulfurization

F. J. Pérez-Reina, E. Rodríguez-Castellón, and A. Jiménez-López*

Departamento de Química Inorgánica, Cristalografía y Mineralogía, Facultad de Ciencias, Universidad de Málaga, 29071 Málaga, Spain

Received October 16, 1998. In Final Form: January 4, 1999

Chromia-pillared α-zirconium phosphate materials have been prepared by two different methods: series a, using as precursor a preswelled phosphate prepared by neutralization up to 70% of the exchange capacity with *n*-propylamine in aqueous solution, and series b, preswelling the phosphate with *n*-propylamine vapors up to saturation. Sulfidation of the pillared materials with a H_2S mixture at 673 K did not result in the formation of isolated chromium sulfide phases but in partial sulfided chromium-oxide-pillared phosphate. The catalysts have been characterized by nitrogen adsorption, X-ray photoelectron spectroscopy (XPS), and oxygen chemisorption. After sulfidation, the modification of textural parameters observed was negligible and slightly different in both series, probably due to higher sulfidation in the pillars of series b. The higher dispersion of chromia in materials of series b detected by XPS was corroborated by the oxygen chemisorption study of the sulfided-pillared materials. Sulfur is found to be present as S^{2-} species. The sulfided catalysts exhibited a high activity and stability for thiophene hydrodesulfurization (HDS), particularly the sulfide−CrZrP-3b material, which, despite its deactivation, after 6 h on stream is very active. However, the oxidic pillars showed an unusual activity, similar to those of sulfided materials. So, the chromia-pillared catalysts, above all those of series b, do not need the initial sulfidation to achieve a considerable activity. The optimal sulfidation temperature and reaction temperature was 673 K. The thiophene hydrodesulfurization exclusively gives rise to the formation of butane and butenes. The constants for hydrogenation of butenes to *n*-butane have also been calculated.

Introduction

There has been a growing need to develop catalysts that can carry out deep hydrodesulfurization (HDS) in order to produce cleaner diesel fuels, because current and future regulations are and will be more restrictive. Preservation of the atmospheric environment is imperative to continue enjoying a healthy life. As crude oils usually contain fairly large amounts of sulfur compounds, it is of great importance to effectively remove sulfur from petroleum products. For this purpose, catalysts play a very important role in hydrotreatment of petroleum fractions.[1] Sulfide catalysts are of great current industrial interest because they are widely used in petroleum refining for hydroprocessing applications such as hydrodesulfurization. In most cases, sulfided catalysts used in industry are derived from oxides of elements of group 6 (Mo or W), group 9 (Co), and group 10 (Ni) supported on different compounds, although the most commonly used is alumina.[2−7] Catalytic activity is related to the presence of sulfides of group 6 and group 9−10 elements; however, the most important role of these last elements is to act as promoters. Many reviews show that transition metal sulfides supported on zeolites are more active in hydrodesulfurization than those supported on silica−alumina or alumina.[8−18]

Pillared layered materials present some properties similar to those of the zeolites.[19] Their pore structure and catalytic behavior can be controlled, with aproximate precision, depending on the size and type of the intercalated inorganic oligomeric cation and the degree of intercalation. These materials are formed by incorporation of oligomeric hydroxocations into the interlayer region of bidimensional inorganic solids (e.g., clays, metal(IV) phosphates, etc.). After calcination at 673−773 K, the materials contain metal oxides that, acting as pillars, maintain the layers permanently separated. The cavities thus formed can be easily accessible to different adsorptives. When pillared materials are partially sulfided, the overall pillared structure is maintained and a unique catalytic microenvironment is created. There are not much data about metal sulfides supported on pillared clays and phosphates. Burch and Warburton[20] prepared stable iron

(1) Ozaki, H. *Catal. Surveys Jpn.* **1997**, *1*, 143−155.
(2) Weisser, O.; Landa, S. *Sulfide Catalysts, Their Properties and Applications*; Pergamon: New York, 1973.
(3) Massoth, F. E. *Advances in Catalysis and Related Subjects*; Academic Press: New York/London, 1978; Vol. 27, p 265.
(4) Delmon, B. *Proceedings, 3rd International Conference on Chemistry and Uses of Molybdenum*, Ann Arbor, 1979; Barry, H. F.; Mitchell, P. C. H., Eds.; Climax Molybdenum Co.: Ann Arbor, 1979; p 73.
(5) Grange, P. *Catal. Rev. Sci. Eng.* **1980**, *21*, 135.
(6) Gates, B. C.; Katzer, J. R.; Schuit, G. C. A. *Chemistry of Catalytic Processes*; Mc-Graw Hill: New York, 1979; p 390.
(7) Cid, R.; Neira, J.; Godoy, J.; Palacios, J. M.; López-Agudo, A. *Appl. Catal. A* **1995**, *125*, 169.
(8) Cid, R.; Orleans, F.; Lopes-Aged, A. *Appl. Catal.* **1987**, *32*, 327.
(9) Fierro, J. L. G.; Conesa, J. C.; López-Agudo, A. *J. Catal.* **1987**, *108*, 334.
(10) Cid, R.; Fierro, J. L. G.; López-Agudo, A. *Zeolites* **1990**, *10*, 95.
(11) Anderson, J. A.; Pawelec, B.; Fierro, J. L. G.; Arias, P. L.; Duque, F.; Cambra, J. F. *Appl. Catal.* **1993**, *99*, 55.
(12) Kovacheva, P.; Davidova, N.; Novakova, J. *Zeolites* **1991**, *11*, 54.
(13) Laniecki, M.; Zmierczak, W. *Zeolites* **1991**, *11*, 18.
(14) Laniecki, M.; Zmierczak, W. *Zeolites Chemistry and Catalysis*; Jacobs, P. A., et al., Eds.; Studies in Surface Science and Catalysis Vol. 69; Elsevier: Amsterdam, 1991; p 331.
(15) Leglise, J.; Janin, A.; Lavalley, J. C.; Cornet, D. *J. Catal.* **1988**, *114*, 388.
(16) Ezzamarty, A.; Catherine, E.; Cornet, D.; Hemidy, J. F.; Janin, A.; Lavalley, J. C.; Leglise, J. *Zeolites, Facts, Figures, Future*; Jacons, P. A., et al., Eds.; Studies in Surface Science and Catalysis Vol. 49; Elsevier: Amsterdam, 1989; p 1025.
(17) Welters, W. J. J.; Korànyi, T. I.; de Beer, V. H. J.; van Santen, R. A. *New Fronters in Catalysis*; Guczi, L., et al., Eds.; Elsevier: Amsterdam, 1993; Vol. 75, p 1931.
(18) Welters, W. W. J.; Vorbeck, G.; Zandbergen, H. W.; de Haan, J. W.; de Beer, V. H. J.; van Santen, R. A. *J. Catal.* **1994**, *150*, 78.
(19) Vaughan, D. E. W.; Lussier, R. J.; Macgee, S. L., Jr. U.S. Patent 4,176,090, 1979.

10.1021/la981446k CCC: $18.00
Published on Web 02/24/1999

sulfide-pillared montmorillonite, being active catalysts in hydrotreating reactions.[21] Later, Occelli and Rennard[22] used an alumina-pillared bentonite as a support for a Ni−Mo catalyst for hydrogenation−hydrocracking of vacuum gas oil feedstocks. Kloprogge et al.[23] prepared a supported nickel sulfide on alumina pillared montmorillonite which exhibited high activity for HDS of thiophene. Recently, Mérida-Robles et al.[24] have shown that fluorinated alumina-pillared α-zirconium phosphate materials are appropriate supports for preparing sulfided catalysts. The Ni−Mo-based catalysts are highly dispersed and present high activity due to the promoter effect of Ni. Chromia-pillared montmorillonite exhibits a high activity and selectivity in cyclohexane dehydrogenation, hydrocracking of *n*-decane, cumene conversion, and toluene disproportionation.[25−28] Sychev et al.[29] described that chromia-pillared clay activated with an H_2S-H_2 mixture displayed interestingly high activity for thiophene HDS and consecutive hydrogenation of butene. Given that α-ZrP is an appropriate matrix to prepare pillared materials with high surface areas and porosity in which the nanoparticles of chromia are highly dispersed between the layers,[24] it should be of great interest to investigate the properties of chromia-pillared α-zirconium phosphate in the hydrodesulfurization process.

In fact, in a previous study,[30] we described a new method for preparing colloidal suspensions of α-zirconium phosphate, based on the use of a phase preswelled with *n*-propylamine vapors. This intercalate is spontaneously exfoliated in contact with a weakly acidic aqueous solution. The intercalation of Cr^{3+} oligomers in this colloidal phosphate is higher than that in a colloidal phosphate obtained by a conventional method.[31] The new chromia-pillared materials displayed a remarkable acidity, and the effect of the chromium content and chromia dispersion will be studied in the catalytic behavior for the thiophene HDS reaction.

Experimental Section

Material Preparation. Two series of chromia-pillared α-zirconium phosphates (α-ZrPs) were synthesized as described elsewhere.[30] For this purpose, colloidal suspensions of this phosphate were prepared by two different methods, hereinafter called series a and series b. The preparation of series a consists of adding dropwise a 0.1 M *n*-propylamine (nPA) aqueous solution to a suspension of α-ZrP under vigorous stirring up to pH = 8 (70% of the cation exchange capacity (CEC) of α-ZrP). Preparation of series b makes use of a fully saturated nPA intercalate as intermediate. A typical preparation of the colloidal phase is as follows: α-ZrP (2 g) was exposed to nPA vapors overnight, and once the excess amine was removed, in a desiccator containing concentrated phosphoric acid, the intercalate obtained was dispersed in 400 cm^3 of a 0.03 M aqueous solution of acetic acid (in these conditions, the phosphate was neutralizated to 80% of the CEC). Subsequently, the pH was raised to 8 with a 0.1 M nPA aqueous solution.

The colloidal suspensions a and b were separately contacted with chromium acetate aqueous solutions (Carlo Erba), in which the $[Cr^{3+}]$ varied from 0.015 to 0.031 M. The mixtures were refluxed for 4 days. After reaction, the green solids were recovered by centrifugation, washed three times with deionized water, and dried at 333 K. The two series of oligomeric chromium(III)-intercalated materials are designated hereinafter as CrZrP-*X*a and CrZrP-*X*b, where *X* is related to the chromium content. Chromia-pillared materials were obtained by calcining the intercalated precursor materials at 673 K under nitrogen flow. The calcined samples were washed with distilled water before characterization.

For the preparation of a K^+-exchanged sample, an ammonia-exchanged sample was obtained by exposing the calcined sample to a flow of NH_3 at 373 K for 1 h to neutralize even the weakest acid sites. The solids were then dispersed for 15 h in a 0.1 M solution of potassium acetate.The resulting exchanged sample was washed with deionized water and dried at 673 K for 1 h.

Chemical Analysis and Characterization. Chemical analysis of intercalated precursor materials was carried out after digestion of samples with a $NaOH/H_2O_2$ solution. Chromium was determined colorimetrically using the chromate method (λ = 372 nm). XRD of cast films, dried at 333 K or calcined at different temperatures, was performed with a Siemens D501 diffractometer, provided with a graphite monochromator and using Cu Kα radiation. XPS analysis was obtained with a Physical Electronics 5700 instrument with a Mg Kα X-ray excitation source ($h\nu$ = 1253.6 eV) and a hemispherical electron analyzer. Accurate (±0.1 eV) binding energies (BEs) were determined with respect to the position of the C 1s peak at 284.8 eV. The residual pressure in the analysis chamber was maintained below 10^{-9} Torr during data acquisition. Adsorption−desorption of N_2 on the oxidic and sulfide samples (77 K, outgassing at 473 K and 10^{-4} Torr overnight) was measured on a conventional volumetric apparatus. The assessment of the micropore volume (*t*-plots) was carried out using a CrZrP material calcined at 1073 K as reference, which is a nonporous solid with a S_{BET} of 34 $m^2\ g^{-1}$. Oxygen chemisorption was performed to determine the dispersion of the active phase using a conventional volumetric apparatus. For this purpose, 0.450 g of sample was sulfided in situ following the same procedure as that for the activity measurements. After sulfidation, the catalysts were flushed for 1 h at 673 K in helium and outgassed overnight. Then, the sample was cooled to 248 K, at which temperature the oxygen chemisorption was performed. The range of pressure studied in chemisorption was 0−450 Torr, and the amount of oxygen chemisorbed was calculated by extrapolation of isotherms at $P = 0$. In the same experimental conditions, consumption of oxygen was zero on oxidic pillars.

Catalytic Activity Measurements. The catalysts were tested in the thiophene hydrodesulfurization reaction at 673 K, using an automatic microcatalytic flow reactor under atmospheric pressure. The catalysts were supported between quartz wool in a quartz tube reactor. The catalyst charge used was 0.2 g without dilution. The catalysts were heated (673 K) under He flow and previously sulfided in situ in a flow of 60 $cm^3\ min^{-1}$ H_2S/H_2 (10% H_2S) using the following temperature program: 10 K min^{-1} increases from room temperature to 673 K and keeping the catalysts for 1 h at 673 K. After sulfidation, the gas flow was switched to the reactor: a hydrogen flow of 50 $cm^3\ min^{-1}$ containing 4.0 mol % thiophene. The contact time was 0.15 g s mol^{-1}, and catalysts did not show diffusion restrictions. The reactor effluents were sampled via a microvolume sampling valve and injected into a gas chromatograph equipped with a flame ionization detector (FID) and a capillary column (TBR-1). On the basis of conversion data and assuming that reactions are pseudo-first-order, the rate constant for HDS (k_{HDS}) was calculated at different reaction times by the equation $k_{HDS} = F/W(\ln 1/(1-x))$, where *W* is the catalyst weight, *F* is the feed rate of thiophene, and *x* is the fractional conversion. The selectivity for hydrogena-

(20) Burch, R.; Warburton, C. I. *J. Chem. Soc., Chem. Commun.* **1987**, 117.
(21) Warburton, C. I. *Catal. Today* **1988**, *2*, 271.
(22) Occelli, M. L.; Rennard, R. J. *Catal. Today* **1988**, *2*, 309.
(23) Kloprogge, J. T.; Welters, W. J. J.; Booy, E.; de Beer, V. H. J.; van Sante, R.; Geus, J. W.; Jansen, J. B. H. *Appl. Catal. A* **1993**, *97*, 77.
(24) Mérida-Robles, J. M.; Rodríguez-Castellón, E.; Olivera-Pascual, P.; Jiménez-López, A. *J. Mol. Catal.*, in press.
(25) Tzou, M. S.; Pinnavaia, T. J. *Catal. Today* **1988**, *2*, 243.
(26) Bradley, S. M.; Kydd, D. A. *J. Catal.* **1993**, *141*, 239.
(27) Bradley, S. M.; Kydd, D. A. *J. Catal.* **1993**, *142*, 448.
(28) Auer, H.; Hofmann, H. *Appl. Catal.* **1993**, *97*, 23.
(29) Sychev, M.; de Beer, V. H. J.; van Santen, R. A.; Prohod'ko, R.; Goncharuk, V. *Zeolites and Related Microporous Materials: State of the Art 1994*; Weitkamp, J., Karge, H. G., Pfeifer, H., Hölderich, W., Eds.; Studies in Surface Science and Catalysis Vol. 84; Elsevier: Amsterdam, 1994; p 267.
(30) Pérez-Reina, F. J.; Olivera-Pastor, P.; Rodríguez-Castellón, E.; Jiménez-López, A. *Langmuir* **1998**, *14*, 4017.
(31) Maireles-Torres, P.; Olivera-Pastor, P.; Rodríguez-Castellón, E.; Jiménez-López, A.; Tomlinson, A. A. G. *J. Mater. Chem.* **1991**, *1* (5), 739−746.

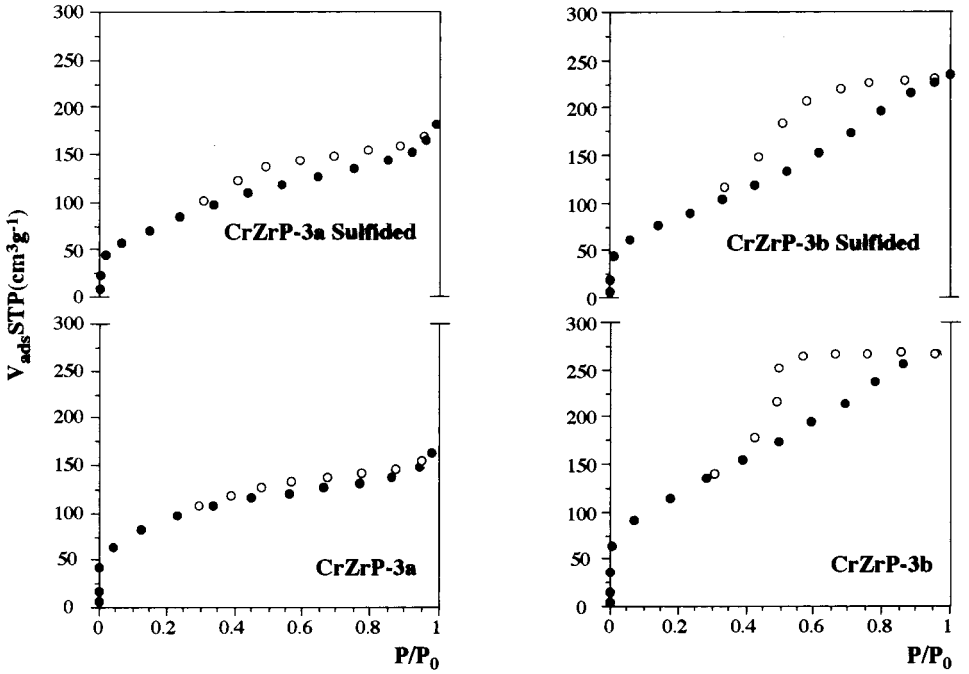

Figure 1. Typical N_2 adsorption−desorption isotherms (77 K) for chromia-pillared materials and sulfided materials.

Table 1. Chemical Composition and d_{001} Basal Spacing of Polyhydroxyacetate Cr^{3+} Intercalates and Chromia-Pillared α-Zirconium Phosphate

sample	% Cr in precursor	Cr_2O_3/α-ZrP molar ratio	d_{001} (Å) (room temp)	d_{001} (Å) (673 K)
CrZrP-1a	18.2	0.95	20.1	11.4
CrZrP-2a	21.4	1.50	28.3	amorphous
CrZrP-3a	23.1	1.90	35.5	27.0
CrZrP-1b	16.7	0.93	22.1	amorphous
CrZrP-2b	21.6	1.60	30.2	amorphous
CrZrP-3b	25.2	2.72	44.0	30.0

tion (HYD) of butenes to butane, expressed as the ratio k_{HYD}/k_{HDS}, was calculated according to the method of Okamoto et al.[32]

Results and Discussion

Characterization of Catalysts. It has been demonstrated, from a previous study,[30] that the porous structure and the surface reactivity of chromia-pillared α-zirconium phosphate are clearly determined by the preparation conditions of these materials. In particular, the method of colloidization of the starting phosphate controls the final porous texture of the resulting pillared materials because not only some surface characteristics of the host matrix but also the nature of the intercalated chromium(III) oligomers and the content of space filling molecules (water + organic matter) are modified by the colloidization procedure. Thus, two different series of chromia-pillared materials, designated hereinafter as CrZrP-*X*a and CrZrP-*X*b, are investigated in connection with the HDS catalytic activity.

The composition and XRD data for all materials are compiled in Table 1. The oligomeric species intercalated into colloidal α-ZrP were Cr(III) polyhydroxoacetate clusters with a nuclearity which depends on the chromium concentration in the solution and the colloidization method. According to precedent X-ray absorption spectroscopy (XAS) studies,[33] the XRD data are compatible with the presence in the phosphate interlayer region of bilayers of trimers (samples 1a and 1b), trimers + tetramers (2a and 2b), tetramers,[3a] and possibly higher oligomers for materials 3b. Although well-defined species are intercalated into the phosphate, calcination leads to a decrease of the basal spacing due to dehydration and partial dehydroxylation of the intercalated oligomers and a progressive loss of long range order. Thus, the XRD patterns of the materials calcined at 673 K showed a very broad signal, corresponding to the d_{001} basal spacing, or in some cases, it was absent. However, no evidence of layer collapse was found in any samples, or for the crystalline phases, the free heights (estimated by subtracting from the basal spacing the thickness of the phosphate layer, 6.3 Å) varied between 5.1 and 23.7 Å. The disorder caused by the heat treatment seems to be a general behavior of oxide-pillared phosphates, which may be attributed to the appearance, upon dehydration, of face-to-edge and edge-to-edge particle packet interactions, in detriment to face-to-face interactions, predominant in the intercalates at room temperature. These modifications in the phosphate layer stacking, after calcination at 673 K, originate a mixed micro- + mesoporous structure in all chromia-pillared materials, as will be shown.

In fact, the N_2 adsorption−desorption isotherms (Figure 1), at 77 K, correspond to solids with a mixed porosity, with V_{micro} (*t*-method) ranging between 0.16 and 0.25 cm^3 g^{-1}. The isotherms are indicative of the existence of mesoporosity, as shown by the hysteresis loop. This type of hysteresis is characteristic of materials with platelike texture.[34] It is generally accepted that the microporosity is induced by pillaring;[35] therefore, the high microporosity of these materials is related to the presence of chromia pillars in the interlayer space. Relevant textural parameters are listed in Table 2. In both series of pillared materials, the porosity increases with the chromium content; thus, sample 3b exhibits the highest specific

(32) Okamoto, Y.; Katon, Y.; Mori, Y.; Imanaka, T.; Teranishi, S. J. *J. Catal.* **1980**, *66*, 93.

(33) Jones, D. J.; Roziere, J.; Maireles Torres, P.; Jiménez López, A.; Olivera Pastor, P.; Rodríguez Castellón, E.; Tommlinson, A. A. G. *Inorg. Chem.* **1995**, *34*, 4611.

(34) Gregg, S. J.; Sing, K. S. W. *Adsorption Surface Area and Porosity*, 2nd ed.; Academic Press: New York, 1982; p 221.

(35) Sterte, J.; Otterstedt, J. E.; Thulin, H.; Massoth, F. E. *Appl. Catal.* **1988**, *A38*, 119.

Table 2. Textural Parameters of Chromia- and Sulfided-Chromia-Pillared α-Zirconium Phosphate Materials

material	S_{BET} ($m^2\ g^{-1}$)	$V_{\mu p}$[a] ($cm^3\ g^{-1}$)	$\sum V_{ac}$[b] ($cm^3\ g^{-1}$)	$2t$[a] (Å)
CrZrP-1a	64	0.03	0.06	11.1
CrZrP-1b	265	0.18	0.31	13.1
CrZrP-2a	262	0.14	0.19	9.2
CrZrP-2a sulf	221	0.11	0.17	11.1
CrZrP-2b	357	0.18	0.39	12.2
CrZrP-2b sulf	224	0.10	0.39	13.7
CrZrP-3a	319	0.17	0.23	10.5
CrZrP-3a sulf	288	0.16	0.27	11.3
CrZrP-3b	426	0.25	0.44	12.0
CrZrP-3b sulf	308	0.17	0.38	12.9

[a] Obtained from *t*-plot. [b] Calculated from Cranston−Inkley method.

surface area and the highest micropore volume. Another important observation from this study is that the porosity, both micro- and mesoporosity, is higher for materials of series b, as compared with the homologous materials of series a. This effect is a direct consequence of the greater degree of delamination produced when method b is used, which leads to a higher amount of space-filling matter in the interlayer region and an increase in the edge-to-face and edge-to-edge interactions of the platelets.

After sulfidation, the BET surface area decreases by about 15% and 9% for samples 2a and 3a, respectively, while the diminution is more marked for samples 2b and 3b, being 37% and 28% respectively. The diminution of the micropore volume in the case of sulfided CrZrP compared to that for chromia-pillared materials indicates that formation of the chromium sulfide phase takes place inside the porous structure of the chromia-pillared materials. The BET surface area decrease is mainly due to a decrease in the micropore volume (Table 2). Therefore, it may be deduced that sulfidation occurs preferentially in micropores located in the interlayer region, as a result of the reaction between the surface of chromia pillars and the sulfuring agent. This also means that sulfidation is produced to a greater extent in materials of series b; nevertheless, the sulfided chromia-pillared compounds still maintain high porosity, as S_{BET} and V_{micro} were higher than 200 $m^2\ g^{-1}$ and 0.1 $cm^3\ g^{-1}$, respectively. On the other hand, the width of the slit-shaped pores (which are characteristic of pillared clays[29]) can be estimated from the inflection point in the *t*-plot. Twice this *t*-value[2t] is assigned to an approximate slit width of the pores.[36] Malla and Komarneni[37] suggested that a change of the lateral pillar spacing leads to the increase/decrease of pore slit width. Hence, it is reasonable to suppose that the different amount of pillars in CrZrP materials influences their pore slit width. In each series, material 2 presents a lower content of chromium than material 3; however, only in series b do $2t$ values decrease with the chromium content (higher pillar density). In all cases, after sulfidation, the $2t$ values increase. This behavior has also been observed in chromia-pillared montmorillonites.[38]

Consequently, taking into account these results, one can conclude that sulfidation does not alter drastically the pore structure of chromia-pillared α-zirconium phosphate and so the catalysts exhibit an attractive design to be used in hydrodesulfurization reactions.

Table 3. Binding Energies (eV) of Chromia- and Sulfided-Chromia-Pillared α-ZrP Materials

pillared material		BE (eV) O 1s	BE (eV) Cr $2p_{3/2}$	BE (eV) S 2p	atomic ratio on surface Cr/Zr	atomic ratio on surface S/Cr	atomic ratio on surface O/Cr
CrZrP-3a							
	pillar	531.0	576.9		2.84		4.31
	sulf pillar	531.4	577.0	162.2	2.79	0.12	4.51
	sulf pillar[a]	531.5	577.1	161.8	2.68	0.06	4.62
	pillar[a]	531.5	577.0	161.4	2.73	0.03	4.64
CrZrP-3b							
	pillar	531.0	576.8		3.73		3.45
	sulf pillar	531.3	577.0	161.8	3.28	0.19	3.74
	sulf pillar[a]	531.4	577.0	161.2	3.27	0.23	3.75
	pillar[a]	531.5	577.0	161.5	3.60	0.13	4.10

[a] After hydrodesulfurization reaction.

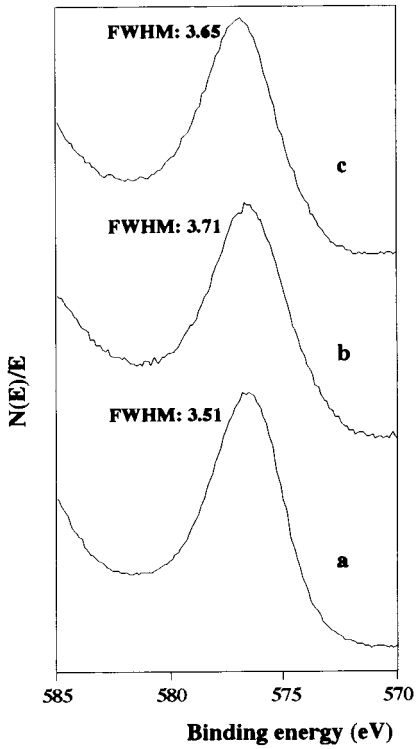

Figure 2. Cr $2p_{3/2}$ XPS spectra of CrZrP-3b material: (a) pristine pillared material; (b) sulfided pillared material; (c) spent sulfided pillared material.

The XPS technique was used to investigate the changes of the immediate environment surrounding chromium and the oxidation state of chromium upon sulfidation as well as after the catalytic reaction. In Table 3 the binding energies of the core levels Cr $2p_{3/2}$, O 1s, Zr $3d_{5/2}$, and P 2p are compiled for pillared and sulfided pillared CrZrP-3a and CrZrP-3b materials. The binding energies of Cr $2p_{3/2}$ in the pillared materials (576.8−576.9 eV) are coincident with those reported for chromia (576.7−576.9 eV),[39] and therefore only Cr(III) is present in the oxide-pillared phosphate (Figure 2). No appreciable changes were observed in either series of materials, except that the Cr 2p/Zr 3d and O 1s/Cr 2p ratios were variable according to chromium content and the polymerization degree of the intercalated species. After sulfidation, the position of Cr $2p_{3/2}$ remained practically unshifted although

(36) Yamanaka, S.; Takahama, K. In *Multifunctional Mesoporous Inorganic Solids*; Sequeira, C. A. C., Hudson, M. J., Eds.; Kluwer: Dordrecht, 1993; p 237.

(37) Mulla, P.; Komarneni, S. In *Proceedings of the 9th International Clay Conference*, Strasbourg, 1989; Farmer, V. V., Tardy, Y., Eds.; *Sci. Geol., Mem.* **1990**, *86*, 59.

(38) Sychev, M.; de Beer, V. H. J.; Kodentsov, A.; van Oers, E. M.; van Santen, R. A. *J. Catal.* **1997**, *168*, 245.

(39) Moulder, J. F.; Stickle, W. F.; Sobol, P. E.; Bomben, K. D. In *Handbook of X-ray Photoelectron Spectroscopy*; Chastain, J., Ed.; Perkin-Elmer: Minneapolis, MN, 1992; p 213.

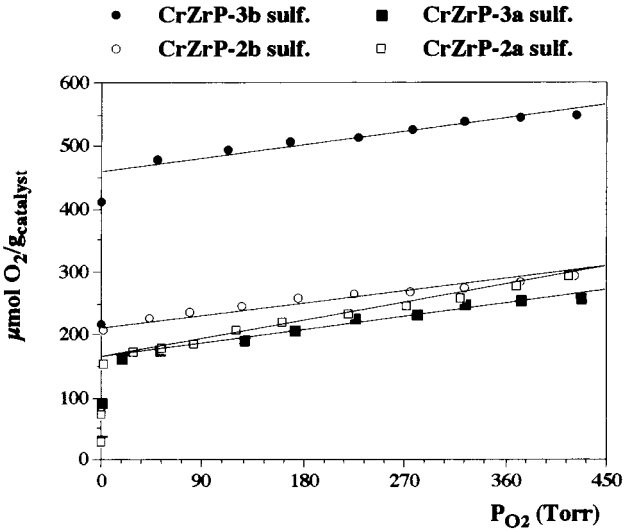

Figure 3. O_2 chemisorption isotherms (248 K) for different sulfided chromia pillared materials.

Table 4. Oxygen Uptake at 248 K by Sulfided Chromia-Pillared α-ZrP Materials

sample	O_2 chemisorbed (μmol g^{-1}_{catal})
CrZrP-2a sulf	160
CrZrP-3a sulf	166
CrZrP-2b sulf	224
CrZrP-3b sulf	472

the fwhm was larger and, moreover, the S 2p/Cr 2p found was extremely low (Table 3). These results suggest that sulfided chromia located inside micropores could not contribute to the signal of sulfided catalysts.

In contrast, the S 2p/Cr 2p ratio was 1.25 for sulfided-chromia-pillared montmorillonite.[38] In such a system, sulfidation also causes a shift of the binding energy of Cr $2p_{3/2}$ to a lower energy (576.0 eV). Regarding the chromium dispersion, sulfidation only gave rise to a slight decrease of the Cr 2p/Zr 3d ratio, which means that the chromium pillars remain in practically the same location after the H_2S treatment. The binding energy values of S $2p_{3/2}$ for the sulfided samples were in the range 161.8−162.2 eV, which is lower than that expected for chromium sulfide (162.5 eV) and slightly higher than the value reported for S^{2-} ions (161.0−161.7 eV),[40,41] possibly indicating that the formation of a superficial mixed oxide−sulfide of chromium(III) takes place. Evidence for the presence of elemental sulfur (164.4 eV) or sulfate ions (169.0 eV) was not found. On the other hand, the peak positions of Cr $2p_{3/2}$ and S $2p_{3/2}$ in the XPS spectrum of sulfided pillared materials indicate that no segregated phases of chromium sulfide were formed upon sulfidation.

The O_2 chemisorption isotherms for the sulfided pillared materials have been obtained to ascertain information about the dispersion of the active phase. All isotherms are of the Langmuir type (Figure 3). The oxygen amount chemisorbed is compiled in Table 4. These values were obtained by extrapolation to $P = 0$ Torr. No chemisorption was observed for the oxidic pillars at this temperature (248 K). In sulfided pillared materials of series a, the oxygen amount retained was very similar, but in those of series b, this amount was higher and the variation is more pronounced with chromium content. So, the dispersion of the active phases is higher in the sulfided pillared materials of series b than that of the analogous ones in series a. This result is very important because the dispersion of the active phase is a critical factor in the catalytic process. This behavior also reveals the importance of method b in the preparation of pillared materials where a more homogeneous distribution of pillars between layers is attained.

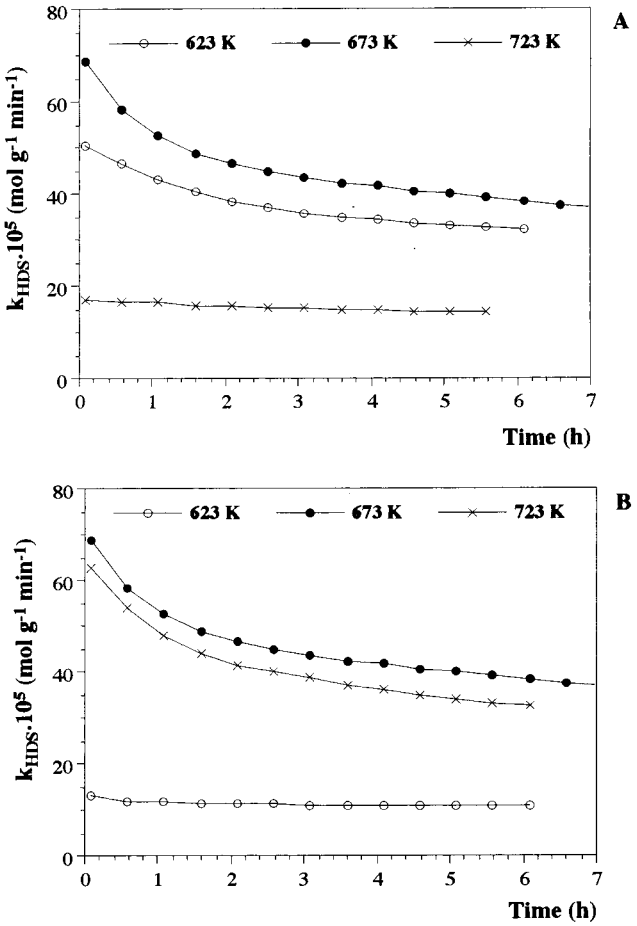

Figure 4. Dependence of the catalytic activity on sulfidation temperature (A) and reaction temperature (B) for sulfided chromia-pillared materials.

Catalytic Activity in Thiophene HDS. The thiophene HDS reaction has been used to establish the activity of the sulfided pillared materials. Previously, a study has been carried out to establish the optimum sulfidation temperature and reaction temperature. For this purpose, the CrZrP-3b catalyst has been chosen.

The catalytic activity depends on the sulfidation temperature (Figure 4A; reaction temperature 673 K). The activity increases with the activation temperature up to 673 K. A further increase of temperature provokes a decrease in the catalytic activity. The highest activity was obtained when the sulfidation temperature was 673 K. At 623 K, the activity was slightly lower, but at 723 K the activity decreased drastically, probably due to a sinterization of the active phase. This behavior has been observed in other catalysts described in the literature.[42−44] The sulfidation temperature influences the reaction

(40) De Jong, A. M. Thesis, Eindhoven University of Technology, Eindhoven, 1994.
(41) Bouwer, S. M. A. M.; van Zon, F. B. M.; van Dijk, M. P.; van der Kraan, A. M.; de Beer, V. H. J.; van Veen, J. A. R.; Koningsberger, D. C. *J. Catal.* **1994**, *146*, 375.
(42) Arteaga, A.; Fierro, J. L. G.; Delannay, F.; Delmon, B. *Appl. Catal.* **1986**, *26*, 227.
(43) Henriques, C. A.; Bentes, A. M. P.; Frety, R.; Schmal, M. *Catal. Today* **1989**, *5*, 443.
(44) Texeira da Silva, V. L. S.; Fety, R.; Schamal, M. *Ind. Eng. Chem. Res.* **1994**, *33*, 1692.

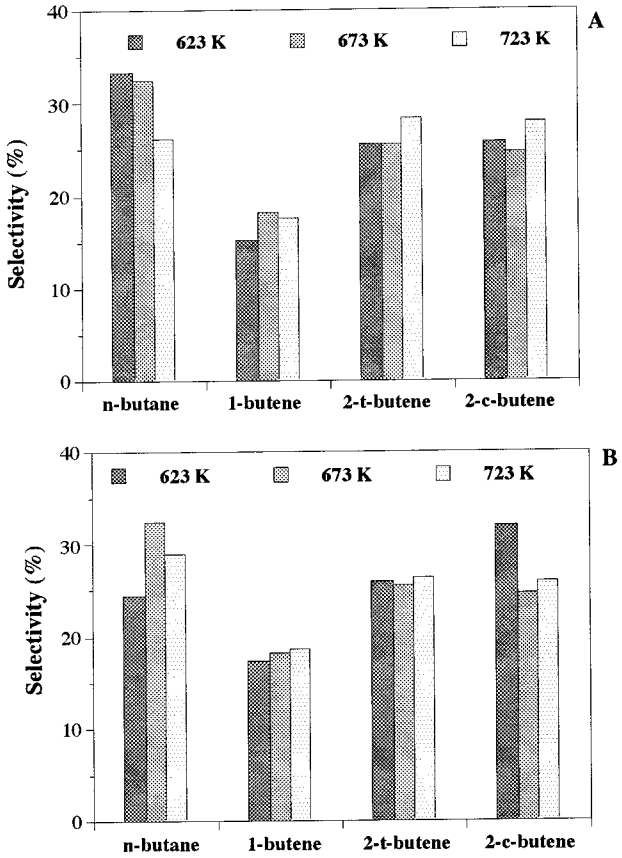

Figure 5. Product selectivities on thiophene HDS as a function of sulfidation temperature (A) and reaction temperature (B).

products too. Thus, the selectivity for *n*-butane decreased with increasing sulfidation temperature (Figure 5A).

Furthermore, the HDS reaction temperature has been examined (Figure 4B; sulfidation temperature 673 K). Again, the activity was maximum at 673 K. However, the activity was now lowest at 623 K, although no deactivation was observed. In this case, the highest selectivity through *n*-butane was at 673 K (Figure 5B). As a results of these findings, the optimum sulfidation and reaction temperature was found to be 673 K. Thus, all catalysts were tested for thiophene HDS at this temperature.

Figure 6 shows the catalytic activity for different sulfided pillared materials versus time on stream. In Table 5 these values are compiled at 5 and 300 min. In each series, the activity is related with the chromium content present in the catalysts. Sulfided CrZrP-1a and CrZrP-1b were not active in this process, possibly due to the low content and dispersion of chromium in both materials. In comparison, catalysts of series b are more active. Sulfided CrZrP-3b displayed the highest initial activity, although exhibiting a low decay in the activity with the time on stream due to coking. Nevertheless, this catalyst still showed an activity after 6 h about three times superior to that of its homologue in series a.

With respect to selectivity, other products apart from butane and butenes were not detected. Only during the initial stage of the catalytic test at 673 K were small amounts (less than 5%) of C_1-C_3 hydrocarbons detected when the sulfided-CrZrP-3b catalyst was tested. In Figure 7 the distribution of the reaction products is shown. The majority of products was 2-*trans*/*cis*-butene, except in sulfided-CrZrP-3b, where the most abundant product was *n*-butane. No tetrahydrothiophene (THT) or butadiene was detected due to their high reactivity in the experimental conditions. The catalytic behavior shown by these catalysts

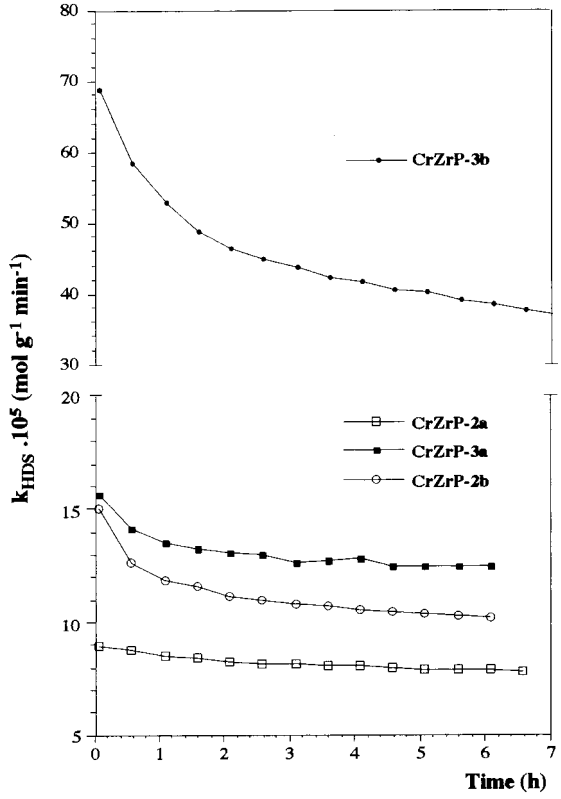

Figure 6. Thiophene HDS activity for sulfided-chromia-pillared catalysts.

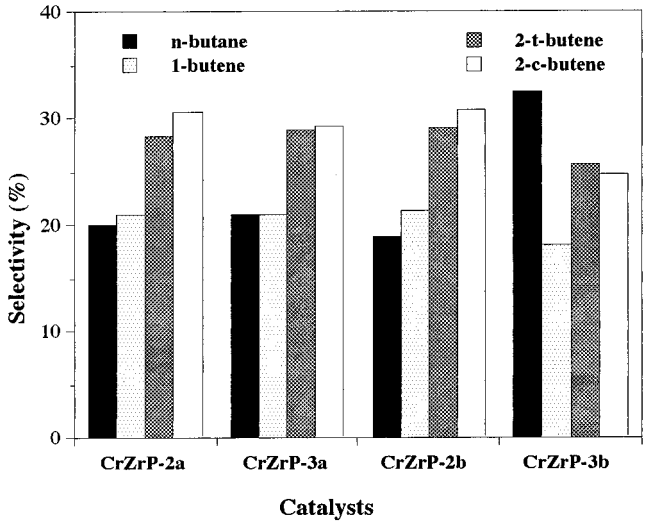

Figure 7. Product selectivities of thiophene HDS reaction for both series of sulfided materials at 673 K.

Table 5. Catalytic Activity for Thiophene Hydrodesulfurization (HDS) and Subsequent butene Hydrogenation (HYD) of Sulfided Pillared Materials

	$10^5 k_{HDS}$ (mol g^{-1} min^{-1})		$10^5 k_{HYD}$ (mol g^{-1} min^{-1})	
pillared material	5 min	300 min	5 min	300 min
CrZrP-2a sulf	8.9	7.9	9.0	9.0
CrZrP-3a sulf	15.6	12.5	10.0	9.0
CrZrP-2b sulf	15.0	10.2	8.6	8.1
CrZrP-3b sulf	68.6	38.3	15.0	11.1
K^+-CrZrP-3b sulf	10.8	9.5	13.1	12.4

can be explained by means of two factors: dispersion of the active phase and the acidity of the catalysts. The sulfided-CrZrP-3b catalyst displayed the highest dispersion, as deduced from the O_2-chemisorption data. Besides,

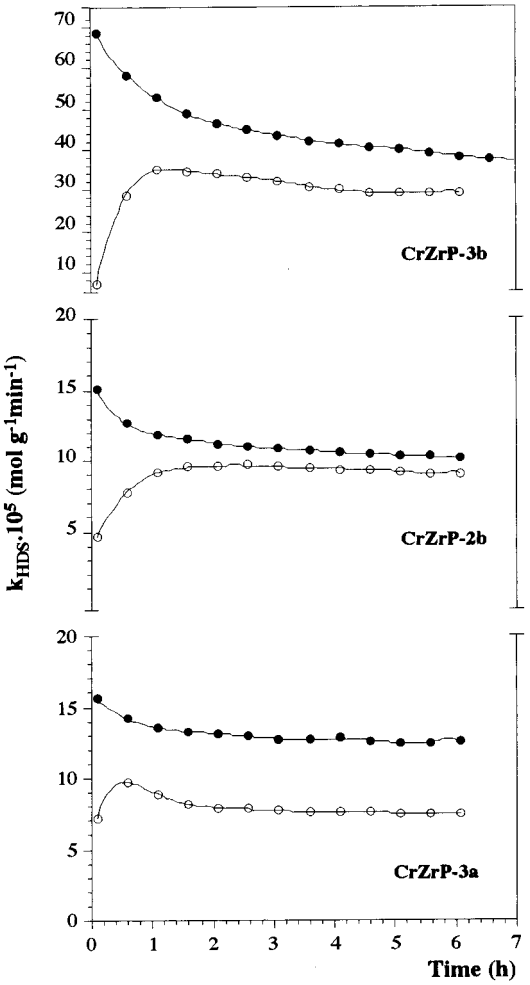

Figure 8. Comparative thiophene HDS over sulfided (●) and nonsulfided (○) pillared materials.

CrZrP-3b showed a considerable acidity, as measured by NH_3-TPD (2.35 mmol g^{-1}) and 2-propanol decomposition, with an activity of 17.4 μmol g^{-1} s^{-1}.[30] To evaluate the acidity effect in this reaction, a K^+-CrZrP-3b material was used as catalyst. As expected, the acidity of this doped catalyst is lower than that of CrZrP-3b due to the ionic exchange between H^+ and K^+.[30] The activity found for the thiophene hydrodesulfurization of this sulfided K^+-CrZrP-3b catalyst was four times lower than that observed in the pristine. So, it can be assumed that the acidity is another important factor influencing the DHS reaction, as has been pointed out by Welter et al.[45]

To evaluate the influence of the sulfidation process of catalysts, the oxide-pillared materials were tested in the HDS reaction. When a CrZrP material is subjected to this process, the initial activity is minimal, but it increases with time on stream up to obtaining a value slightly lower than that observed with the sulfided pillar homologue (Figure 8). In the catalysts of series b, the sulfidation and activity are higher, which is in good agreement with the better dispersion of chromium observed from O_2 chemisorption data. These findings suggest that, during reaction, the chromia-pillared material is autosulfided by means of S coming from thiophene. This process increases to reach its highest activity after 120−150 min of reaction. This seems to confirm the mechanism of hydrodesulfurization

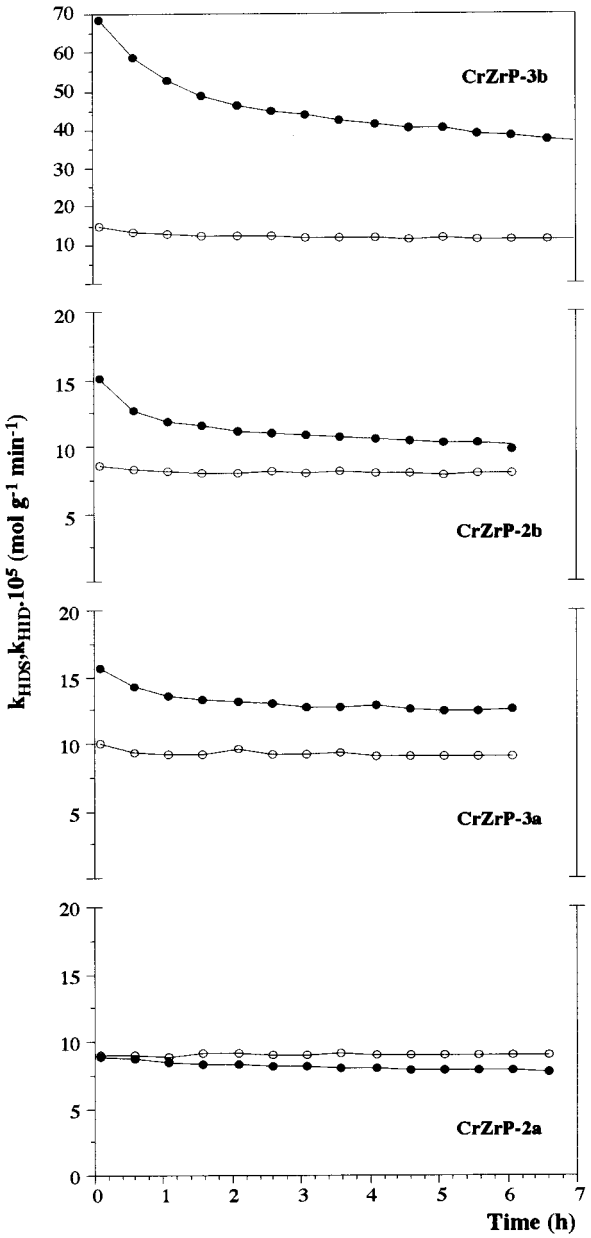

Figure 9. Comparative k_{HDS} (●) and k_{HYD} (○) over sulfided pillared materials.

proposed by Kabe et al.,[46−49] who concluded that sulfur in the reactive (thiophene) is not directly released as hydrogen sulfide but previously incorporated into the catalysts. This result is very important because the chromia-pillared phosphate materials do not need, above all in series b, a previous sulfidation to achieve high activity in the catalytic process for thiophene hydrodesulfurization. In this case, the observed selectivity is similar to that obtained with sulfided catalysts, but in the former the selectivity to *n*-butane is slightly higher. After DHS reaction, the pillared materials contain sulfur with the same BE and similar S/Cr as those observed for sulfided pillared materials (Table 3). The same behavior was observed in nonsupported chromia catalysts.[50]

(45) Welters, W. J. J.; de Beer, V. H. J.; van Santen, R. A. *Appl. Catal. A* **1994**, *119*, 253.
(46) Kabe, T.; Qian, W.; Ogawa, S.; Ishihara, A. *J. Catal.* **1993**, *143*, 239.
(47) Qian, W.; Ishihara, A.; Ogawa, S.; Kabe, T. *J. Phys. Chem.* **1994**, *98*, 907.
(48) Kabe, T.; Qian, W.; Ishihara, A. *J. Phys. Chem.* **1994**, *948*, 912.
(49) Kabe, T.; Qian, W.; Ishihara, A. *J. Catal.* **1994**, *149*, 171.
(50) Owens, P. J.; Amberg, C. H. *Can. J. Chem.* **1962**, *40*, 941.
(51) Kolboe, S. *Can. J. Chem.* **1969**, *47*, 352.

The activity that nonsulfided catalysts have shown cannot be explained according to what has been stated above (synergic effect between acidity and sulfided active phase). This activity, in acidic catalysts, is probably carried out in Brønsted centers.[50] After the autosulfidation process, the formation of SH groups takes place around the active sites. As the SH concentration increases, the activity rises. At the beginning of the reaction, there is no previous sulfided phase, and so it is probable that the thiophene molecule holds in a coordination unsaturated sites of an active chromium. During this stage, no H_2S is removed because it is used to sulfide the chromia pillars, until reaching a saturated state, which must be coincident with the highest activity. So, the formed SH groups produce an important synergic effect with the metallic sites.

In this study, the hydrogenation process of butenes to *n*-butane has also been calculated. Figure 9 shows that k_{HYD} is generally lower than k_{HDS}, but it remains constant during reaction. The k_{HYD} values obtained were of the same order for all catalysts, and a similar behavior was detected with nonsulfided catalysts (not shown).

Conclusions

Intercalation of polyhydroxoacetate chromium oligomers in α-ZrP and subsequent calcination at 673 K under nitrogen give rise to the formation of porous materials with high surface areas. Two series of chromia-pillared phosphate are prepared from two colloidal suspensions obtained through different methods. The higher dispersion of chromium in materials of series b displayed a superior activity for the thiophene hydrodesulfurization. Data from nitrogen adsorption, XPS analysis, and oxygen chemisorption reveal that sulfided materials b show a higher sulfidation degree and very good dispersion in the active phase. The optimum sulfidation and reaction temperature was 673 K, although some deactivation was detected. The catalyst with the highest activity was sulfided CrZrP-3b. It is important to emphasize that oxide-pillared materials showed a significant activity for thiophene HDS due to experimenting with an important autosulfidation. These chromia-pillared materials displayed a moderate activity for the hydrogenation of butenes.

Acknowledgment. This research was supported by the CICYT (Spain) Project MAT 97-906.

LA981446K